POLYPUBLIE

Universal short time g*-functions : generation and application

Michel Bernier, Yves Brussieux

Document en libre accès dans PolyPublie
Open Access document in PolyPublie

Date	2019
Type	Article de revue / Article
Version	Version finale avant publication / Accepted version
URL de PolyPublie PolyPublie URL	https://publications.polymtl.ca/4088/
Évaluation par les pairs Peer reviewed	Révisé par les pairs / Refereed
Conditions d'utilisation Terms of use	© Tous droits réservés / All rights reserved
Référence Citation	Bernier, M., & Brussieux, Y. (2019). Universal short time g*-functions : generation and application. Science and Technology for the Built Environment, 25(8), 993-1006. https://doi.org/10.1080/23744731.2019.1648132

Publication officielle
Official publication

Titre de la revue Journal title	Science and Technology for the Built Environment (vol. 25, no. 8)
Maison d'édition Publisher	Taylor & Francis
URL officielle Official URL	https://doi.org/10.1080/23744731.2019.1648132
Mention légale Legal notice	This is an Accepted Manuscript of an article published by Taylor & Francis in Science and Technology for the Built Environment (vol. 25, no. 8) in 2019, available online: https://doi.org/10.1080/23744731.2019.1648132

Ce fichier a été téléchargé à partir de PolyPublie, le dépôt institutionnel de Polytechnique Montréal
This file has been downloaded from PolyPublie, the institutional repository of Polytechnique Montréal
https://publications.polymtl.ca



Science and Technology for the Built Environment

ISSN: 2374-4731 (Print) 2374-474X (Online) Journal homepage: https://www.tandfonline.com/loi/uhvc21

Universal short time g*-functions: generation and application

Yves Brussieux & Michel Bernier

To cite this article: Yves Brussieux & Michel Bernier (2019): Universal short time g*-functions: generation and application, Science and Technology for the Built Environment, DOI: 10.1080/23744731.2019.1648132

To link to this article: https://doi.org/10.1080/23744731.2019.1648132

Accepted author version posted online: 31 Jul 2019.

Submit your article to this journal

View Crossmark data

Full Terms & Conditions of access and use can be found at
https://www.tandfonline.com/action/journalInformation?journalCode=uhvc21

Check for updates

Universal short time g*-functions: generation and application

Yves Brussieux, Michel Bernier

Ecole Polytechnique de Montreal, Montreal, Quebec, Canada

Corresponding author Michel Bernier michel.bernier@polymtl.ca

Accepted Manuscript

ABSTRACT

A hybrid numerical/analytical one-dimensional model is proposed to predict the thermal behavior of borehole heat exchangers in the short period following a step change in operating conditions. Transient heat transfer in the borehole is solved numerically using an equivalent composite cylinder geometry while ground heat transfer is evaluated analytically using the infinite cylindrical heat source solution. The proposed model is then used to generate C-functions, which are based on a slightly different definition than the traditional g-functions. For short times, C-functions depend on four non-dimensional parameters: t Ł G4 , P P (with P equal to a new characteristic time) and 0 and 0 , non-dimensional parameters related to the fluid and the ground, respectively. A set of universal C-functions curves generated with the proposed model is presented. Then, these curves are used in a borehole sizing problem. It is shown that the inclusion of borehole thermal capacity has a direct effect on the daily and monthly effective ground thermal resistances which reduces the required borehole length by a few percent.

Keywords geothermal; g-functions; Thermal capacity

INTRODUCTION

So-called g-functions are used extensively in the design and simulation of vertical ground heat exchangers

(VGHE). g-Functions are thermal response factors that give the non-dimensional temperature drop at the borehole wall due to a constant total heat extraction rate in a borehole field. Traditional (or long-time) g-functions depend on four non-dimensional parameters: P ,Pthe non-dimensional time, with P L 6{ , the characteristic time of the bore field and the ground thermal diffusivity; N * the non-dimensional borehole radius; $ * the bore field aspect ratio; and & * the non-dimensional buried depth of the boreholes. As shown in Figure 1, g-function curves are typically plotted as a function of H:JP P). For large values of H:JP P), g-function curves depend largely on the non-dimensional borehole spacing, $ *. These curves merge into a single curve with a decrease in the value of H:JP P). The original (or long-time) g-functions obtained by Eskilson (1987) did not cover time periods of less than a month. As reported by Yavuzturk and Spitler (1999), Hellström extended the g-functions so that they could be used down to about 100 hours. For a typical borehole, this represents a value of H:JP P; N9. It is possible to extend g-function curves below this value using the infinite line source solution for example. One such curve (indicated by an arrow for $ * L ») is presented in Figure 1. However, this curve does not account for short-time transient effects due to the borehole thermal capacity.

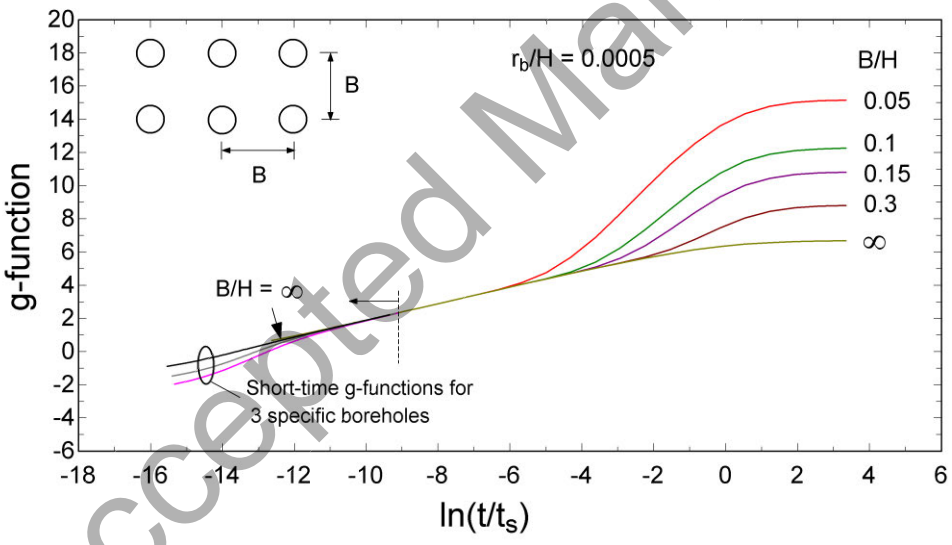


Figure 1 Short-time and long-time g-functions on the same non-dimensional time scale

Yavuzturk and Spitler (1999) were the first to extend the concept of g-functions to short time steps taking into account the pipe and grout thermal capacities but neglecting the fluid thermal capacity. Xu and Spitler (2006) extended this work by approximating the U-tube geometry with a series of hollow cylinders representing the fluid, the internal convective resistance, the pipe, the grout and the ground. They have shown that results obtained with

Accepted Manuscript

this technique compare favorably well with the ones obtained with a two-dimensional model representing the real borehole geometry. Brussieux and Bernier (2018) followed a similar approach for the borehole but used the cylindrical heat source solution to model transient effects in the ground. Using this approach, it is possible to calculate g-functions for short times. Three such curves are presented in Figure 1 for H:P P; O9. These curves are specific to certain borehole characteristics and are plotted using the same non-dimensional scale used for long-time g-functions.

In this paper, it is shown that it is possible to obtain universal short-time g-functions using four non-dimensional parameters: tŁG4 , P P, 0 , 0 . To avoid confusion with the standard g-function definition, the name has been changed to C-function. However, C-function are identical to standard g-functions for long times. Typical C-function curves are presented in Figure 2. Note that short-time C-functions use the top scale based on H:P P; while long-time C-functions (to the right of the vertical line) use the bottom scale based on H:P P;. The objective of this paper is to show how to generate these universal short-time C-function curves and to provide an example of their application.

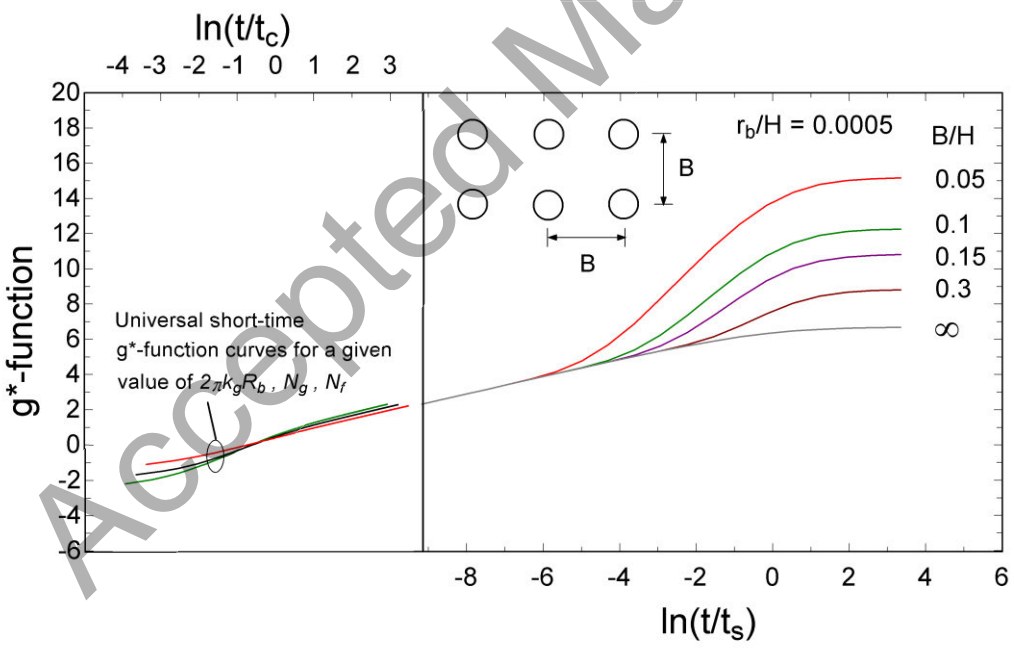


Figure 2 Schematic representation of universal short-time -function curves along with traditional long-time g-function.

Accepted Manuscript

LITERATURE REVIEW

The impact of borehole thermal capacity on borehole heat transfer has been the subject of many investigations. Shirazi and Bernier (2013) provided a thorough review of the area up to 2013. Other studies, which were not reviewed by these authors, will now be discussed.

Yavuzturk et al. (2009) improved the approach developed by Yavuzturk and Spitler (1999) mentioned earlier. Their proposed model is one-dimensional (in the radial direction) and couples two different calculation domains. First, heat transfer in the borehole is solved with a finite element method where the borehole wall temperature is considered to be known. Secondly, ground heat transfer is solved with an analytical short time response factor based on the infinite cylindrical heat source. At each time step, an iterative method gives the fluid temperature based on the wall temperature obtained at the previous time step. The equivalent geometry used is the one developed by Gu and O'Neal (1998) except that the borehole thermal resistance is evaluated using the multipole method. The model is implemented in TRNSYS and validated against numerical and analytical models as well as experimental data. The model proposed here is based on a similar approach except that the equivalent geometry is different as well as the solution methodology. In addition, the proposed model goes one step further by proposing a method to generate and use short time C-functions.

Javed et al. (2010), Javed and Claesson (2011) and Claesson and Javed (2011) proposed an analytical one-dimensional model to simulate the short and long term thermal response of VGHE where the U-tube is replaced by a composite cylinder. Borehole heat transfer is solved in the Laplace domain with the use of a circuit of thermal resistances and then inverse transforms are used to revert back to the time domain. Lamarche (2015) used a similar approach and later used his solution to study the impact of short time effects on the required length of VGHE (Lamarche, 2016). He showed that for a particular case, the required borehole length could be overestimated by about 5% when short-term effects are neglected.

Li and Lai (2013) and Li et al. (2014) proposed a two-dimensional analytical model for U-tube boreholes in which each tube is replaced by an infinite line source. Their results match experimental data with good accuracy for times as short as several minutes. Ma et al. (2015) used a similar composite-medium line source but in three dimensions to account for the variation of fluid temperature along the U-tube. However, the fluid thermal capacity is not taken into account in these models.

Accepted Manuscript

Yang and Li (2014) proposed a new two-dimensional finite volume model considering the fluid capacity and used it to validate the previously developed composite medium line source model (Li and Lai, 2013) which did not consider fluid and pipe heat capacities. When compared with the sand box dataset of Beier (Beier et al. 2011), it is shown that the two models match very well except in the first minutes where the heat capacity affects the results. The influence of other parameters like shank spacing or thermal properties is also studied and once again, the two models differ only during the first minutes.

Li and Lai (2015) provided a discussion on several new advances of borehole heat exchangers analysis. A critical review of six analytical models is presented. The difficulty in providing a precise heat transfer model which covers different time scales is emphasized. Numerical model can be very precise, but they are computationally intensive and thus cannot be used efficiently for long simulations. Analytical models do not suffer from long computations but are based on more stringent assumptions which may limit their accuracy. Aside from the reference dataset of Beier et al. (2011), the authors also note the lack of experimental data to validate models.

Li et al. (2017) proposed a new VGHE sizing equation taking into account the short-term thermal resistance and variation in the fluid temperature. The new effective thermal resistance is divided into a fluid-to-pipe resistance based on the work of Ma et al. (2015) and a pipe-to-ground thermal resistance based on the G-function concept developed by Li et al. (2014). The new sizing equation is compared with the original ASHRAE sizing equation (ASHRAE, 2015) and a simulation-based design tool from Cullin et al. (2015). When compared to the data of Cullin et al. (2015) the new sizing equation appears to be more accurate than the ASHRAE sizing equation. The authors performed a sensitivity study to determine the influence of each parameter on the calculated length. This analysis is particularly relevant when the uncertainty on thermal properties is important. The authors provided G-function curves in the form of G-charts to help the calculation of short time thermal resistances. However, it appears that these charts do not cover all possible borehole configurations and parameters.

De Rosa et al. (2014) compared their short-term Borehole to Ground (B2G) model to the Duct ground heat STorage (DST) model developed by Hellström (1989) and implemented in TRNSYS. The B2G model is based on a two-dimensional thermal resistance-capacity approach including vertical discretization of the borehole. Thermal properties of the pipe, grout and ground are considered but not the fluid capacity. The model is compared with experimental data from an operating ground source heat pump installed to provide heating and cooling of a university building. Results show that the B2G model is more accurate than the DST model for the prediction of the outlet temperature under on/off operating conditions. Ruiz-Calvo et al. (2015) describe more precisely the structure of the B2G model. The model is improved by adding new thermal resistances to better capture the

Accepted Manuscript

thermal interaction between the U-tube legs and convection heat transfer. However, it does not consider the fluid thermal capacity. The model is validated against two different step tests with a 260 m deep water-filled borehole. The tests compare experimental and simulated values of the outlet fluid temperature with a ten-hour heat injection period. Two main adjustment parameters are determined and optimized, the penetration depth and grout node positions. The model is then combined with long term g-functions (Ruiz-Calvo et al., 2016) to obtain a full-time scale model.

Minaei and Marefat (2017a) proposed a simplification to the well-known thermal resistance capacity model, which is based on a stiff system of equation that makes it unstable except for small time steps. In the resulting STRCM model, they merged the two-grout zones proposed in the original version of the model into a single one. When compared with the sand box data of Beier (Beier et al., 2011), the TRCM and STRCM give both accurate results except for very early times where the simplified version is less accurate. However, the loss in accuracy is balanced with a gain in stability since the STRCM model is based on a non-stiff differential equation. A three-dimensional version of the STRCM is also proposed where heat transfer is solved numerically inside the borehole and analytically outside, using the infinite cylindrical heat source solution. The borehole is divided vertically into slices and each slice is solved with the 2D STRCM model. Slices are linked with the corresponding heat flux entering/leaving slices. The simplicity, accuracy and stability of the STRCM model makes it easy to implement into a building simulation software. In a related study, Minaei and Marefat (2017b) used a similar STRCM approach to model heat transfer in a single or double U-tube geometry. Governing equations are solved with Laplace transform and results are compared with the experimental data of Beier (Beier et al., 2011). This model is used to generate short-time g-functions and the influence of several parameters are discussed.

Beier (2014) developed a transient analytical heat transfer model for thermal response tests (TRT). The model uses an equivalent radius to transform the two-pipe geometry into an equivalent cylinder. The equations are solved with Laplace transforms and the vertical temperature profile is also generated. The model is successfully validated against experimental data and it is shown that the vertical temperature prediction capability leads to a more accurate estimation of the borehole thermal resistance than with the traditional mean temperature approximation.

He et al. (2010) studied the difference between two-dimensional and three-dimensional models in the calculation of transient fluid transport and heat transfer in a BHE. They showed that the predictions of transient heat transfer in a borehole from 2D models is not accurate since these models cannot account for fluid transport along the U-tube. Three-dimensional models can alleviate this deficiency, but they are computationally intensive. Instead, the

Accepted Manuscript

authors propose an improved 2D model to reduce computation. This improved model discretizes the borehole into vertical cells with homogenous temperatures, which enables the prediction of the vertical temperature profile and short time non-linearity.

Rees and He (2013) built a 3D numerical model using a finite volume approach to study fluid transport effects for short and long-time scales. The model represents the real borehole geometry including the fluid capacity. It is verified with experimental data obtained at a facility at Oklahoma State University. Emphasis was placed on the study of nonlinearities in temperature and heat flux for short time scales or low flow rates. The model is not convenient to use for any simulation because it is computationally demanding but can be used as a reference to validate other models. Rees (2015) developed an extended two-dimensional model that solves heat transfer in each layer of a VGHE with a finite volume method. This calculation is combined with a pipe model that divides the borehole vertically into small tank volumes. With such divisions, the pipe boundary condition depends on the depth and can reflect the evolution of the fluid temperature along the borehole. The focus of their work is on short-time behavior and thus, grout, pipe and fluid thermal capacities are considered. Different results are compared for the validation against experimental data from Oklahoma State University facility and against a full 3D model. First, the outlet temperature is calculated for varying input temperature based on a sinusoidal profile with a large range of frequencies. For this test, only 3D and extended 2D models are compared. Then, monthly and hourly outlet temperatures are compared between experiments, extended 2D and 3D models. The model shows a good agreement with the 3D model for short times while being more computationally efficient.

Kim et al. (2014) used a hybrid model, numerical inside the borehole and g-functions in the ground, to account for borehole thermal capacity. They used an equivalent radius and a state model size reduction technique to limit computation time. The resulting hybrid-reduced (HR) model was compared to the DST model and with Type451, a double U-tube borehole model that accounts for borehole thermal capacity (Wetter and Huber, 1997). The results obtained with the HR model are in excellent agreement with the DST model in no thermal capacity mode and with Type 451 when thermal capacity is included. However, the HR model involves an elaborate process only applicable to a certain borehole geometry.

Parisch et al. (2015) accounted for the fluid and grout thermal capacities by adding an adiabatic pipe, which accounts for the borehole thermal capacity, upstream of a steady-sate borehole model. Simulations results in TRNSYS performed with this approach show significant improvements.

Biglarian et al. (2017) suggested a numerical model able to predict both short and long-time heat transfer from a single borehole. The inside of the borehole is modeled with a resistance-capacity network, including the fluid

Accepted Manuscript

capacity, and the outside with a finite volume method. A non-uniform grid is used to find a good balance between accuracy and computation time. Results compare favourably well with the experimental data of Beier (Beier et al., 2011), the 3D numerical model of Lee and Lam (2008) and the composite-medium line-source model of Li and Lai (2013).

Nian and Cheng (2018) proposed a new thermal response factor to account for borehole heat capacity. A 1D analytical model transforms the borehole geometry into an equivalent composite cylinder and solves the heat transfer with Laplace transforms. The fluid heat capacity, which is not included at first, is then included with a specific function either for U-tube or coaxial boreholes. The effect of borehole heat capacity and borehole radius on short time g-functions are studied and new g-functions are proposed. They compared favorably well with traditional g-functions and with the experimental data of Beier et al. (2011). However, the influence of conductivities and shank spacing on the response factor is not studied.

As shown by this survey of the literature, there are many ways to model short-time effects associated with borehole thermal capacity. However, unlike the non-dimensional long-time g-function curves, there are no "universal" pre-calculated curves that could be used to account for short-term effects. The objective of this paper is to propose a method to generate such non-dimensional short-time g-function curves.

The paper starts with a presentation of the governing equations and solution methodology followed by a validation of the proposed model against experimental data. Then, the governing non-dimensional parameters for short-time C-function are introduced and universal C-function curves are presented. In the application section of the paper, the ASHRAE sizing equation for VGHE is used in conjunction with short-time C-function to show the impact of borehole thermal capacity on sizing.

PROPOSED MODEL

The following model is based on the equivalent geometry proposed by Xu and Spitler (2006) and illustrated in Figure 3. The two-pipe geometry, with a borehole radius N, is converted into a composite cylinder configuration with the same borehole radius. The outer pipe radius of the equivalent geometry, N Æ Ł , is set equal to t N. This ensures that the volume occupied by the grout is the same in both the real and equivalent geometries.

The inner pipe radius of the equivalent geometry, N ÆÆ, is set equal to N Æ Ł minus the pipe thickness ¿ (L N F N). Then, a mass-less convection layer with a thickness of r t w H ¿ followed by a fully-mixed fluid layer with a thickness of r y w H ¿ are used as suggested by Xu and Spitler (2006). Test performed indicated that

Accepted Manuscript

results were not significantly affected by a variation of these two thicknesses. An additional radius, N, is used by Xu and Spitler (2006) to set the far-field radius in the ground for their numerical model. This radius is not required here since ground heat transfer is handled with an analytical solution. An equivalent fluid thermal capacity, $Ø\,\%\,L_{Æ}$ is determined based on the actual fluid thermal capacity, $Ø\,\%,$ as follows:

$$:Ø\,\%\,L_{Æ}\,L\,\frac{t\,N^{6}_{Æ}}{k\,N^{6}_{ÆÆÆ}\,F\,N^{6}_{Æ}o}\,:Ø\,\%;\qquad(1)$$

The local fluid is at a temperature equal to the average borehole fluid temperature, 6, while the undisturbed ground temperature is given by 6. The steady-state borehole thermal resistance, 4, is equal for both the real and equivalent geometries. It is determined here using the first order multipole method (Hellström, 1991) based on the real geometry. Once the value of 4 is known, each layer is assigned equivalent properties as shown in Table 1.

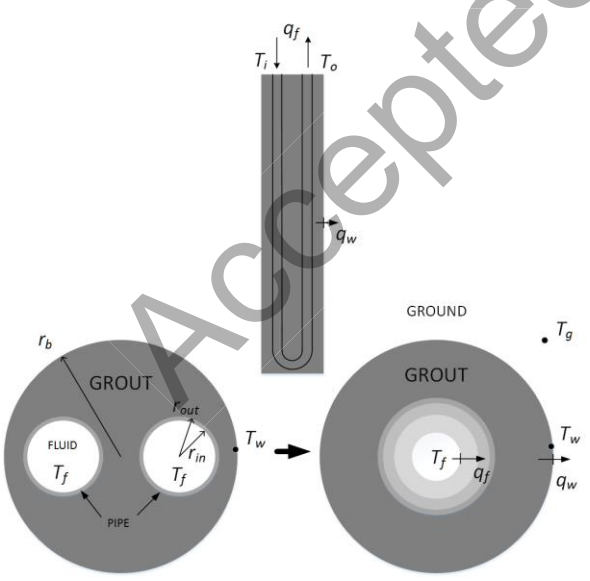
Governing equations and boundary conditions

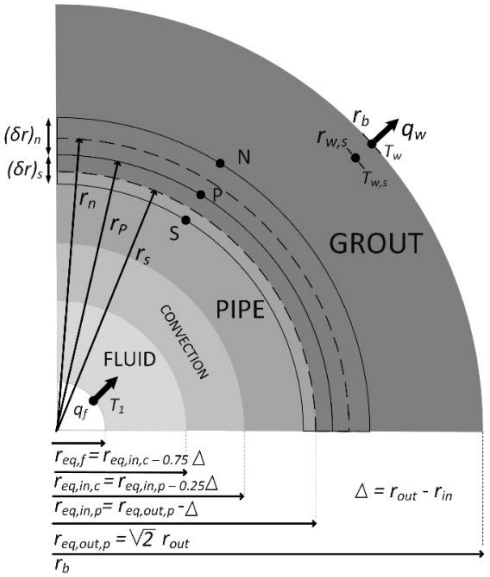
One-dimensional transient heat transfer in the composite cylinder is governed by the following equation:

$$Ø\,\%\,\frac{6}{P}\,L\,G\,\frac{s}{N\;N}\,I\,N\,\frac{6}{IN}\qquad(2)$$

where $Ø$, $\%$ and G are the density, specific heat and thermal conductivity, respectively. This equation is subjected to the following initial and boundary conditions:

$$6_{@4}\,L\;6\qquad 6_{@\sim}\;I\;6_{Æ}:P,\qquad @_{—Æ}\;LMM\qquad(3)$$





Accepted Manuscript

Figure 3 Approximation of the real geometry with an equivalent composite cylinder (left). Dimensions (not to scale) of the various layers and grid layout (right).

Table 1. Equivalent properties for each layer

Layer	Thermal resistance (m-K/W)	Thermal conductivity (W/m-K)	Thermal capacity (¸ o) (kJ/m³-K)
Convection	4 Æ L s / t Ł N Æ D	G Æ L I N ÆÆÆ p / N ÆÆÆ / t Ł 4 Æ / J	Set artificially to a small value
Grout	4 Æ > ª L 4 F ² — Æ ‹ / Æ	G Æ L G Æ ª L I N / N ÆÆÆ p ª / t Ł 4 Æ > ª	Actual thermal capacity
Pipe			Actual thermal capacity
Fluid	negligible	Set artificially to a high value	See equation 1

A M equivalent geometry; ?: convection; C P grout; L pipe; n: number of pipes

Heat transfer in the composite cylinder geometry is solved using the control-volume method of Patankar (1980) with a fully implicit scheme. Using the nomenclature presented in Figure 3, the discretized equation for an internal node P is given by:

$$= 6 \; L = 6 \; E = 6 \; E > \qquad (4)$$

where,

$$= \; L \frac{}{Æ — \; Æ p} \; ; \; = \; L \frac{}{Æ — \; Æ p} ; \; : \; L = 6^{4} \; ; \; = \; L = ^{4} \; E = E = \; ^{4} \; L = \frac{\ldots \; ª \; \cdot \; ? \; \cdot ;}{¿ \; 6}$$

The coefficients = and = , which are different from the traditional formulation given by Patankar (i.e. = L N G : N), are structured so as to account for the logarithmic nature of the temperature profile in a radial configuration. The subscripts 2ÆE and 2ÆW refer to the nodes immediately south and north of node P, respectively. The superscript 0 refers to the previous time step and ¿P is the time step. Control-volume boundaries are placed at the interface of the different cylinders as shown in Figure 3. The size of the control volumes increases exponentially from the interface to the middle of a layer, then decreases symmetrically until the next interface. Such a configuration prevents inconsistencies due to abrupt temperature changes between two adjacent cylinders with different properties.

Accepted Manuscript

At the interface between two different layers, an interface conductivity, $G_{Æ}$ is used between consecutive nodes. For example, for an interface located between nodes P and P,n (with thermal conductivity G and $G_{>5}$ respectively), $G_{Æ}$ is given by:

$$G_{Æ} L GG_{>5}H \frac{H J@\frac{N_{Æ}}{N}A}{G_{>5}H J@\frac{N_{Æ}}{N}A E GH J@\frac{N_{Æ}}{N_{Æ}}A} \quad (5)$$

The boundary condition on the fluid side is entered through the $>$ term for node 6_5:

$$>_5 L =_5 6_5^4 E N_{Æ}M \quad (6)$$

where $M L N_{E}Dk6 F 6_3o$ and D is the internal convection coefficient. Finally, the borehole wall temperature, 6_{CE} is given by the infinite cylindrical heat source solution (ICS) to ground heat transfer obtained at the current time step. The ICS analytical solution requires the heat transfer rate at the borehole wall, M_{CE} This value is obtained from the numerical solution of borehole heat transfer as follows:

$$M_{CE} L F tŁ G_{Æ} \frac{@6}{@N} N F tŁ G_{Æ} \frac{6_{Ù} F 6_{Æ}}{H J\frac{N}{N_{CE}Æ}p} \quad (7)$$

As shown in Figure 3, the subscript $SÆ$ refers to the node immediately upstream of the last node. In turn, the value of M_{CE} is used to obtain the borehole wall temperature using temporal superposition as follows:

$$6_{CE} F 6 L \sum_{@5}^{Æ} IM_{CF Æ} F M_{CE Æ 95} : P F_{?5,}P \quad (8)$$

where J is the total number of time steps, $\grave{}\ L \frac{}{}) : (K;$ and $(_4 L \frac{}{}$

The value of $)$ is the solution of the ICS. A number of approximations for $)$ can be found in the literature; the one provided by Cooper (1976) is used here. The proposed model has been subjected to a grid independence analysis. As reported by Brussieux and Bernier (2018), this analysis indicated that a total of 40 nodes, i.e. 10 nodes per concentric cylinder, and a time step $¿P$ of 0.05 h are required to obtain a grid independent solution.

Comparison with experimental data

The results from the proposed model are compared with the experimental data of Beier et al. (2011). The system parameters, geometry and thermal conductivities are taken from Table 1 of Beier et al. (2011). The specific heat capacities for the fluid, pipe, grout and ground are taken as 4.2, 1.8, 3.8, and 3.2 kJ/kg-K, respectively, based on the work of Minaei and Marefat (2017a). The experimental values of inlet temperatures and flow rates are used as

Accepted Manuscript

inputs to the proposed model. Figure 4 presents the outlet temperature as a function of time predicted by the proposed model and measured by Beier et al. (2011). There is very good agreement between the proposed model and the experiments. The maximum difference is +0.25 K and occurs at the beginning of the test where the outlet temperature experiences a steep change. When averaged for the full test duration the difference is +0.16 K.

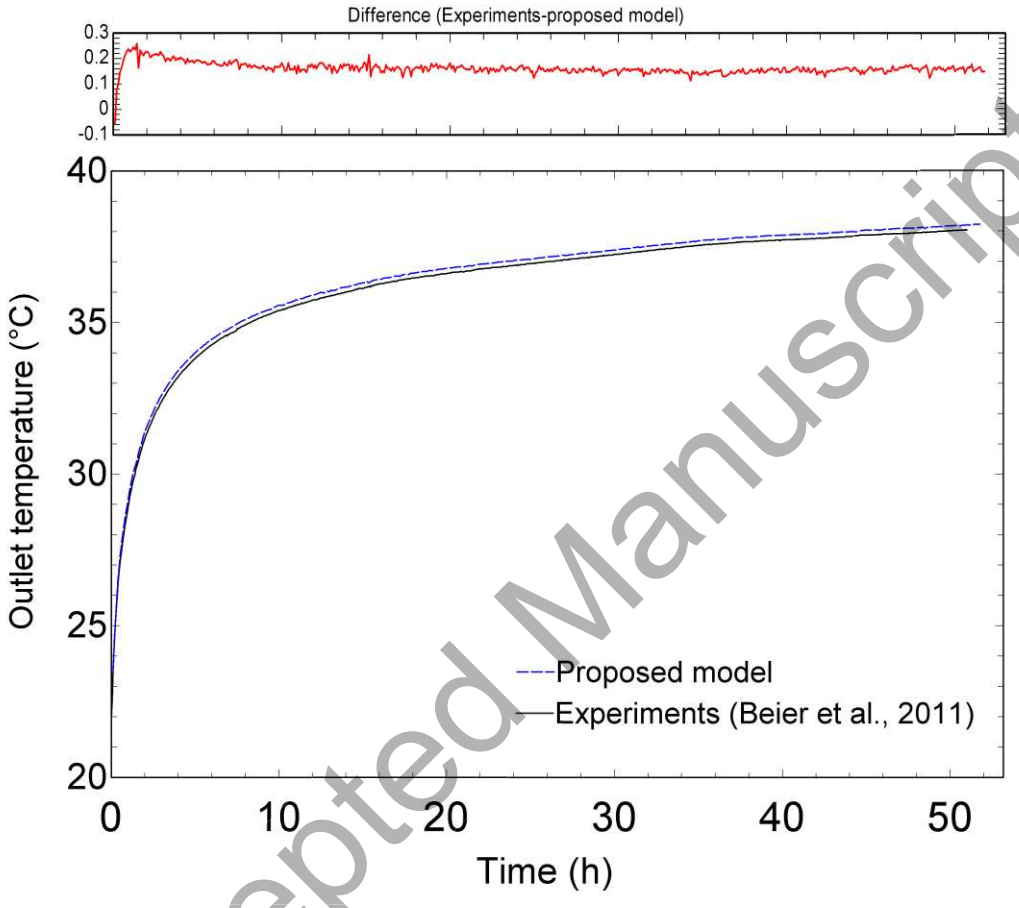


Figure 4 Comparison between the outlet fluid temperature predicted by the proposed model and those measured by Beier et al. (2011).

Accepted Manuscript

Limits of the proposed model

The prediction of the outlet temperature with the proposed model relies on three major assumptions. First, it is a 1D model and only radial heat transfer is considered. Since the proposed model is used here for short operating times (less than ~ 100 hours), longitudinal heat transfer should be negligible (Philippe et al., 2009) so this assumption should not affect the results significantly. The assumption of the single pipe geometry implies that the

thermal short circuit between the two pipes is not considered. The impact of this assumption depends on the borehole size, the flow rate and the fluid temperature. This issue can be partly addressed using an equivalent thermal resistance, R_4 (Javed and Spitler, 2017), which accounts for the thermal short-circuit. Finally, the fluid temperature is assumed to evolve linearly between the inlet and outlet of the borehole. As will be shown shortly the use of R_4 alleviates the deficiencies of this assumption. Rees and He (2013) highlighted the existence of non-linearity in fluid temperature for short times. This non-linearity is mainly due to thermal capacity effects and fluid transport phenomena. In extreme cases, the model can lead to inconsistencies. For example, if the entering fluid temperature increases between two time steps but with a very small flow rate, capacity effects will be dominant, so the fluid temperature in the borehole will not change significantly. However, the model considers that the fluid temperature is the mean of the inlet and outlet temperatures. Consequently, the outlet temperature will decrease by a value equivalent to the inlet temperature increase.

To illustrate the limits imposed by these three assumptions, results from the proposed model are compared with a 2D thermal resistance and capacitance (TRCM) model (Godefroy and Bernier, 2014) for a typical borehole. The TRCM model considers the internal fluid temperature distribution as well as the thermal short circuit and it is used here with a vertical discretization of 10 segments. The ground and borehole temperatures are initially set at 0 °C and the inlet temperature is constant at 30 °C. The borehole length is fixed at 100 m and only the flow rate is varied to modify the residence time of the fluid in the borehole.

Results of this comparison are shown on Figure 5 where the outlet temperature predicted by the two approaches are given for three different fluid replacement rates for a 10-hour simulation period. The fluid replacement rate is defined here as the number of times the fluid is replaced in the entire borehole during a given time step. In other words, it is given by the time step divided by the residence time. Thus, a fluid replacement rate of 1.0 indicates that the fluid has traveled from the inlet to the outlet of the borehole during the calculation time step. Figure 5a uses the traditional borehole thermal resistance, R_4, based on the first order multipole while Figure 5b uses R_4 (Javed and Spitler, 2017).

Accepted Manuscript

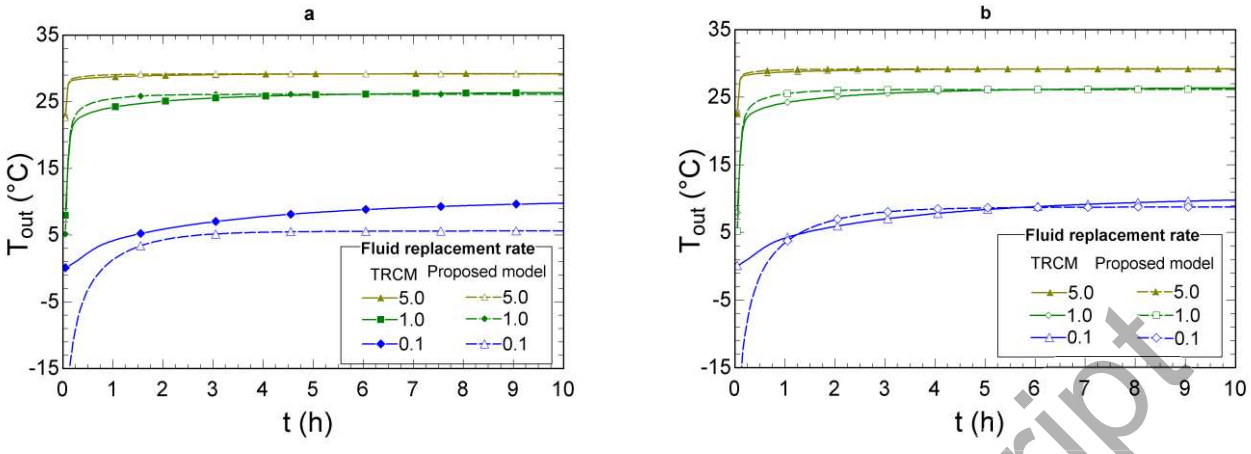


Figure 5 Differences in the prediction of the outlet temperature between the proposed model and a TRCM model. a): using ~ ; b): using ~ .

As shown in Figure 5a, the proposed model is in good agreement with the TRCM model when the fluid replacement rate is above 1.0. For a fluid replacement rate of 0.1, the proposed model is inaccurate for the entire 10 hours of simulation and at P= 10 h, the difference is of the order of 2 K. As explained previously, when the fluid is not renewed at each time step, the mean fluid temperature is not the average between the inlet and outlet temperatures and that causes the outlet fluid temperature to be inaccurate. The second issue which arises for small fluid replacement rates is the thermal short-circuit between the two pipes in the borehole. However, when 4 is used in the model, as shown in Figure 5b, the differences are reduced significantly after the initial period, especially for the cases with the small fluid replacement rates. For example, at P= 10h, and a replacement rate of 0.1, the difference is reduced from to 2.0 K to 0.5 K when 4 is used instead of 4 .

In summary, the proposed model can be inaccurate in the prediction of the outlet fluid temperature when used with deep boreholes and/or low flow rates, i.e. when the fluid replacement rate is small. After the initial transient period, the predictions of the model can be improved if 4 is used in the model. Otherwise, for deep boreholes or low flow rates, the predicted outlet temperature will be irrelevant during the initial transient period when there is a significant change in the inlet temperature. All these issues limit the use of the proposed model for the prediction of the outlet temperature for replacement rate below 1.0. However, the generation of global C- function does not suffer from this limitation as the proposed model is based on the mean fluid temperature not the outlet temperature.

Accepted Manuscript

GLOBAL C-FUNCTIONS

Definition

The original g-functions are response factors used to evaluate ground heat transfer and determine the borehole wall temperature subjected to a constant heat extraction rate. They were not intended to account for transient heat transfer in the borehole and, therefore, are not valid for short operating times. In the approach proposed here, based on the work of Yavuzturk and Spitler (1999), the objective is to obtain the mean fluid temperature in a borehole directly instead of predicting the borehole wall temperature as is the case for traditional g-functions. This translates into the following equation for a constant heat extraction rate M where C-function are used instead of g-function so as to make a distinction with the traditional g-function definition.

$$6 F 6 L M \frac{C}{t Ł G} E 4_{>}; \quad (9)$$

The C-functions for short and long-times are given by:

$$C L \frac{6 \quad K'' ?_{\sim} \quad ?'' o}{} \text{(short-time)} \quad (10)$$

$$C L \frac{6 \quad K'' ?'' o}{} \text{(long-time)} \quad (11)$$

Values of g-functions for long times can either be determined numerically (Eskilson, 1987) or analytically (Cimmino and Bernier, 2013). This typically involves the determination of the borehole wall temperature, 6_{CE} over time for a borehole subjected to a constant heat extraction rate M. Then, Equation 11 is applied to obtain the g-function over time. This leads to curves such as those on the right of the vertical line in Figure 2.

The evaluation of C-functions for short times is based here on the proposed model presented above. The real borehole geometry is converted into an equivalent composite cylinder (Figure 3) with corresponding properties for each layer (Table 1). Then, the proposed model is solved with a constant value of M to obtain the mean fluid temperature, 6. Then C-function are evaluated at each time step using Equation 10. This leads to curves such as those on the left of the vertical line in Figure 2. It should be noted that the term 6 F 4 M in Equation 10 is equal to 6_{CE} when P \» so that values of C-functions calculated using Equations 10 and 11 are identical for long times. However, both equations are used for different purposes, i.e. evaluate 6 and 6_{CE} respectively.

Negative values of -functions

While long-time C-functions are always positive, short-time C-function can take negative values because of the

Accepted Manuscript

subtraction of the 4 M term in Equation 10. For example, Table 2 shows C-functions values obtained with Equation 10 for a typical borehole configuration (characteristics given in Table 3 and 4 L r s m-K/W) with initial fluid and ground temperatures of 0 °C subjected to a heat transfer rate per unit length M= 50 W/m. This table shows the resulting values of 6, M for P= 0.05, 6, 24 and 72 h when using either short or long-time C-functions. For P= 0.05 h, the impact of the heat injection is barely felt at the borehole wall as M has reached a value of 0.9 W/m, approximately 2% of it's steady-state value. This leads to a negative value of - 1.18 for the C-functions and a corresponding value of 6 = 1.09°C. For P= 0.05 h, long-time C-functions are not applicable. For P= 6 h, one may decide to use long-time C-function to obtain 6 using Equation 11 and then 6 using Equation 9. As shown in Table 2, this results in a value of 6 = 10.25 °C which is higher than the value of 6 (8.47 °C) obtained using Equation 10 directly with short-time C-function. This difference decreases with time and is almost negligible for P= 72 h.

	Table 2: -functions for different times				
	Parameter	**=0.05 h**	**=6 h**	**=24 h**	**=72 h**
Using	6 (°C)	1.09	8.47	11.63	13.49
Short-time	M (W/m)	0.9	45.85	49.3	49.78
C-functions	C (-) Equation 10	-1.18	1.04	1.99	2.55
Using	6 (°C)	N/A	10.25	11.69	13.50
Long-time	M (W/m)	N/A	50	50	50
C-functions	C (-) Equation 11	N/A	1.58	2.01	2.55

Non-dimensional parameters for short time -functions

As indicated earlier, long-time g-functions depend on four non-dimensional parameters: P P, N *, $ *, and & *. Short-time C-functions depend on a completely new set of dimensionless parameters.

First, for PL r, 6 = 6 and according to equation 9, C L F t Ł G4 . This is the lower limit of the C- functions and the first non-dimensional parameter. The characteristic time for short time C-functions is defined as:

$$P L \frac{N^{6}}{Æ} L F \frac{:Ø \%; L_{Æ}}{G_{Æ}} G H^{6} N \qquad (12)$$

where the subscript "eq,b" means equivalent borehole and N is the borehole radius. The equivalent borehole thermal diffusivity, Æ is based on the equivalent thermal conductivity, G Æ and equivalent thermal capacitance, :Ø %; L Æ They are defined here as:

Accepted Manuscript

$$G_{\text{æ}} = \frac{H \Downarrow \frac{N}{N_{\text{æææ}}} p}{t \text{Ł} 4} \tag{13}$$

$$:\text{Ø}\%; _{\text{æ}} = \frac{:\text{Ø}\%; _{\text{æ}} k N_{\text{æææ}} F N_{\text{æ}} o E \text{Ø}\%; k N_{\text{æ}} \text{ł} F_{\text{æ}} N_{\text{æææ}} o E \text{Ø}\%; k NF N_{\text{æ}} \text{ł} 9_{\text{æ}}}{N} \tag{14}$$

The equivalent thermal conductivity (Equation 13) is based on the overall borehole thermal resistance, 4 . The equivalent thermal capacitance (Equation 14) is based on a weighted average of the thermal capacitance of each layer.

Figure 6 presents the proposed representation of C-function as a function of H:JP P; First note the lower limit of F t Ł G4 identified earlier. Then, the general behavior of C-functions for short times can be described by two independent regions, called the fluid and the ground domain. All curves in the fluid domain merge to a single value at a pivot point around H:JP P;~ -0.5 and C 1 rwhile curves in the ground domain start at the pivot and then diverge as Pincreases. The value of C L nis interesting from a physical point of view as it implies that 6 F 6 L t Ł G4 M. As shown later in Figure 7, the pivot point location is not always located at (0.5, 0) so it can not be characterized as universal and applicable to any borehole. Investigations are underway to further characterize the pivot point. Curves in both domains are independent from each other; thus, there are actually six different curves in Figure 6.

The curves for small values of H:JP P; depend on the ratio between fluid/pipe and borehole thermal capacities defined as:

$$0 \quad L \frac{t N_{\text{æ}} :\text{Ø}\%;}{:N F t N_{\text{æ}} ;:\text{Ø}\%;} \tag{15}$$

Accepted Manuscript

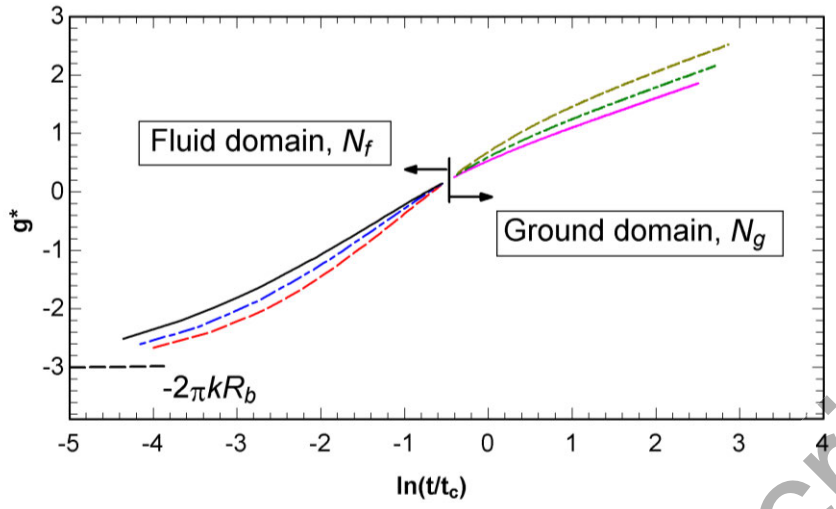


Figure 6 General representaion of short-time -function in the fluid and ground domains

After the pivot point, the fluid capacity effects have disappeared and the curves are now dependent on 0 , the ratio of borehole and ground thermal diffusivities.

$$0 \; L — \; \frac{\left(\; \right)}{:Ø\; ;} \qquad (16)$$

Thus, in summary, C-functions for short times can be fully described with four non-dimensional parameters:

$$C \; L \; Ł \; l \; \frac{P}{P} \; Æ \; t \; Ł \; 4 \; G \; Æ \; Ø Æ \; 0 \qquad (17)$$

A set of universal C-functions curves for short-times are presented in Figure 7. These curves cover the vast majority of typical borehole configurations and can be used along with long-time g-functions as shown in Figure 2 (recall that there are two different characteristic times in Figure 2). For each graph in Figure 7, three different values of 0 and 0 are displayed to cover a wide range of VGHE thermal properties and geometry. Curves are strictly valid only when the flow is turbulent, i.e. for values of D > 500 W/m^2-K.

To use curves presented in Figure 7, the user has to first determine if C-functions curves for short-times should be considered. If the value of H JP P; is lower than -9, then C-function curves for short-times should be used. Then, the graph corresponding to the value of t Ł G 4 has to be selected. Next, based on the value of H JP P; either 0 or 0 needs to be calculated in order to get the value of the C-functions. Finally, equation 9 is used to

Accepted Manuscript

obtain the mean fluid temperature.

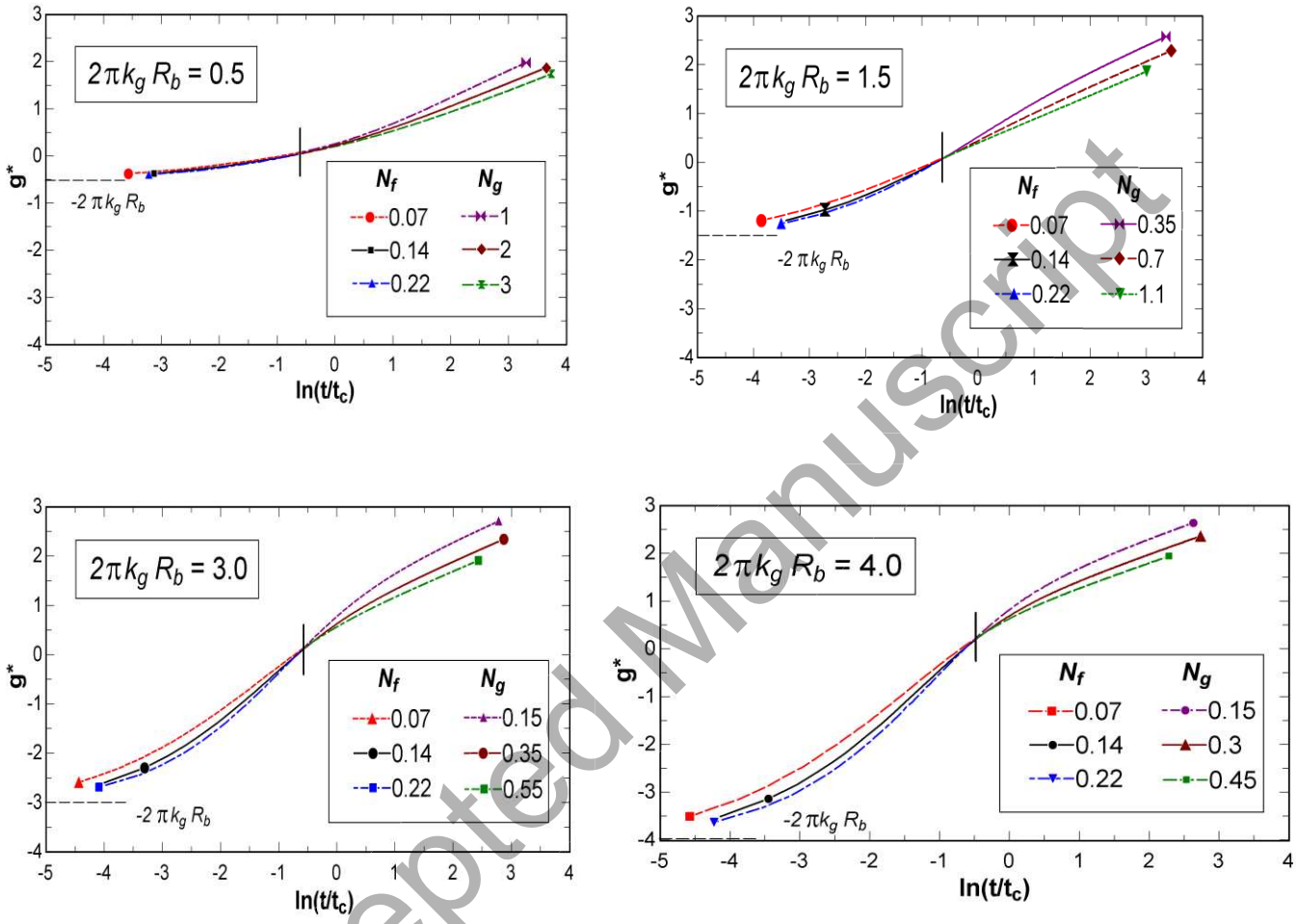


Figure 7 Short-time C-function dataset for four different values of t Ł G4

Accepted Manuscript

Application to the ASHRAE Sizing equation

One of the current ASHRAE sizing equations for vertical boreholes (ASHRAE, 2015) is based on g-functions. It is presented in Equation 18 where the required borehole length, . , is determined using three ground pulses, 3 , 3 and 3 applied over time periods equal to 10 years (P), 1 month (P), and 1 to 6 hours (P), respectively. The denominator corresponds to the temperature difference between the mean fluid

temperature, 6 , and the undisturbed ground temperature, 6 .

$$. L \frac{3\ 4\ \text{Æ}\ E\ 3\ 4\ \text{Æ}\ E\ \ 34\ \text{Æ}\ E\ 3\ 4}{6\ F\ 6} \tag{18}$$

The equivalent ground thermal resistances 4 Æ 4 Æ 4 Æare evaluated as follows (ASHRAE, 2015):

$$L\ B_kC_o\ F\ C_{k\ ?\ .o}OWtŁG\ 4\ \text{Æ}\ L\ B_kC_{?\ .o}\ F\ C_{k\ ?\ .o}OWtŁG\ 4\ \text{Æ}\ L\ B_kC_{?\ .o}OWtŁG \tag{19}$$

where P L P E P E P, P6 L P E P and P5 L P. The subscript " " indicates that the equivalent ground thermal resistances are evaluated using g-functions.

These equations were developed using the common approach of neglecting borehole thermal capacity effects. However, as will now be shown, recalculating the solution with C-functions leads exactly to the same form of the sizing equation.

In general, the difference between the mean fluid temperature and the undisturbed ground temperature for a given heat transfer rate per unit length, M, is given by

$$6\ F\ 6\ L\ \text{¤}\ \tag{20}$$

where ` L —— E 4> Using temporal superposition of the three thermal pulses, it is possible to show that:

$$6\ F\ 6\ L \frac{3\ @\ `kPo\ F\ `kPF\ P_{5o}\ E\ \ ``kPF\ P_{5o}\ F\ `kPF\ P_{6o}\ ?\ E\ `3:P_7\ F\ P_6;}{.} \tag{21}$$

When replacing ` by its value, the borehole thermal resistance term, 4 , cancels out in the annual and monthly terms but it remains in the hourly term. The final expression is:

$$. \frac{3\ 4\ \text{Æ}\ E\ 3\ 4\ \text{Æ}\ E\ \ 34\ \text{Æ}\ E\ 3\ 4}{6\ F\ 6} \tag{22}$$

The corresponding equivalent ground thermal resistances, 4 Æ, 4 Æ, 4 Æ are evaluated as follows:

$$4\ \text{Æ}\ L\ B_kC_o\ F\ C_{k\ ?\ .o}OWtŁG4\ \text{Æ}\ L\ B_kC_{?\ .o}\ F\ C_{k\ ?\ .o}OWtŁG\ 4\ \text{Æ}\ L\ B_kC_{?\ .o}OWtŁG \tag{23}$$

In the end, the equation has exactly the same form as equation 18 except that the original g-functions are replaced by C-functions based on the mean fluid temperature.

It is interesting to examine the impact of short-term effects (borehole thermal capacity) on the required borehole length for a particular example using the methodology proposed here and to make use of the universal curves

Accepted Manuscript

presented in Figure 7. In this example, the required length of a single borehole operating in cooling is required for 3 = 0.5 kW, 3 = 3 kW, and 3 = 9.465 kW and P = 10 y, P =1 month and P = 4 hours, and 6 =35 °C and 6 =13 °C. The other borehole characteristics are given in Table 3. The convective heat transfer, D = 500 W/m^2-K giving a value of 4 = 0.1 m-K/W using the first order multipole method.

Table 3. Borehole characteristics used in the application section

Borehole characteristics		Layer properties		
		Layer	Volumetric heat capacity (kJ/K-m^3)	Thermal conductivities (W/m-K)
Borehole diameter (mm)	108	Fluid	4124	-
U-tube inside diameter (mm)	27.0	Pipe	1540	0.40
U-tube outside diameter (mm)	33.4	Grout	3900	2.32
Shank spacing (mm)	47.1	Ground	2877	2.388

The required length without short-term effects is determined using equation 18. The corresponding g-functions are obtained using the curve for $\$ * L$ »presented in Figure 1 which extends down to H:J/P; L Fs t This curve is only applicable for N *=0.0005, thus for a value of * = 108 m. Therefore, for different values of the N * ratio, the correction factor suggested by Eskilson (1987) is applied as explained by Bernier (2014).

When short-term effects are considered, equation 22 is used where $C_{k\ o}$ and $C_{k\ ?\ o}$ are evaluated using the long-time g-function curve for $\$ * L$,»presented in Figure 1. The term $C_{k\ ?\ o}$ is evaluated using the non-dimensional graphs presented in Figure 7. The solution process is iterative as the required length is not known a priori. Table 4 presents the required borehole length with and without short-term effects and Table 5 presents intermediate values.

Table 4. Short-term effects on borehole length

Parameter	without short-term effects	with short-term effects
Borehole length (m)	102.1	100.0
4 Æ (m-K/W)	0.145	0.145
4 Æ (m-K/W)	0.170	0.178
4 Æ (m-K/W)	0.076	0.069

Accepted Manuscript

Table 5. Parameters used for the short-term calculations		
Parameter	Value	Unit
t Ł G4	1.5	-
G Æ	1.612	W/m-K
:Ø ‰ ; Æ	3.041 H s r·	J/m^3-K
P	5503	s
H JP Ţ	0.9619	-
0	0.6384	-

For this particular example, the design borehole length is slightly oversized by 2.1 % when short-term effects are not taken into account. As noted by Lamarche (2016), short-term g-functions influence the values of 4 Æ and 4 Æ. In this case, the value of 4 Æ decreases by about 11.5 % while the value of 4 Æ increases by about 5%. The percentage of oversizing is problem dependent and it will depend on the relative magnitude between 3 and 3 and the duration of the peak pulse.

To illustrate short-term effects over time, a different calculation is performed with the same three ground pulses. The borehole length is fixed (at 100 m) and the resulting mean fluid temperature is calculated over time for the duration of the three ground pulses with and without thermal capacities. Results of this calculation are shown in Figure 8 where the x-axis is divided into three different time scales representing periods of 10 years, 1 month and 4 hours, respectively.

As indicated in the zoomed graph, there are differences in the mean fluid temperature in the first few hours of the first 10-year period. However, this difference is negligible at the end of the 10-year period as both curves are superimposed. It is also shown that while the heat transfer rate per unit length calculated without thermal capacity is constant, it takes some time for the one calculated with thermal capacity to reach its final steady-state value.

For the second heat pulse, the differences in the value of the mean fluid temperature follow the same pattern, i.e. small differences in the beginning, which become negligible at the end of the period. For the final 4-hour pulse, the mean fluid temperatures calculated with and without thermal capacity give significantly different results. The increase in mean fluid temperature calculated with thermal capacity is more gradual than when thermal capacity is not accounted. At the end of the three pulses, the mean fluid temperature with thermal capacities is lower

Accepted Manuscript

(35.25 °C) than when thermal capacities are not accounted for (36.37 °C). This highlights the positive impact of borehole thermal capacity on sizing. If the fluid temperature is lower for the same heat pulses injected to the ground, it means that the borehole can be shorter to reach the same mean fluid temperature. In fact, this is what the sizing example presented above has shown. The final value of 35.25 °C for g is very close to the value of 35 °C used above in the sizing example. This small difference is attributable to the fact that g-function are interpolated in Figure 7 for the sizing example while direct values issued from the proposed model were used to obtain Figure 8.

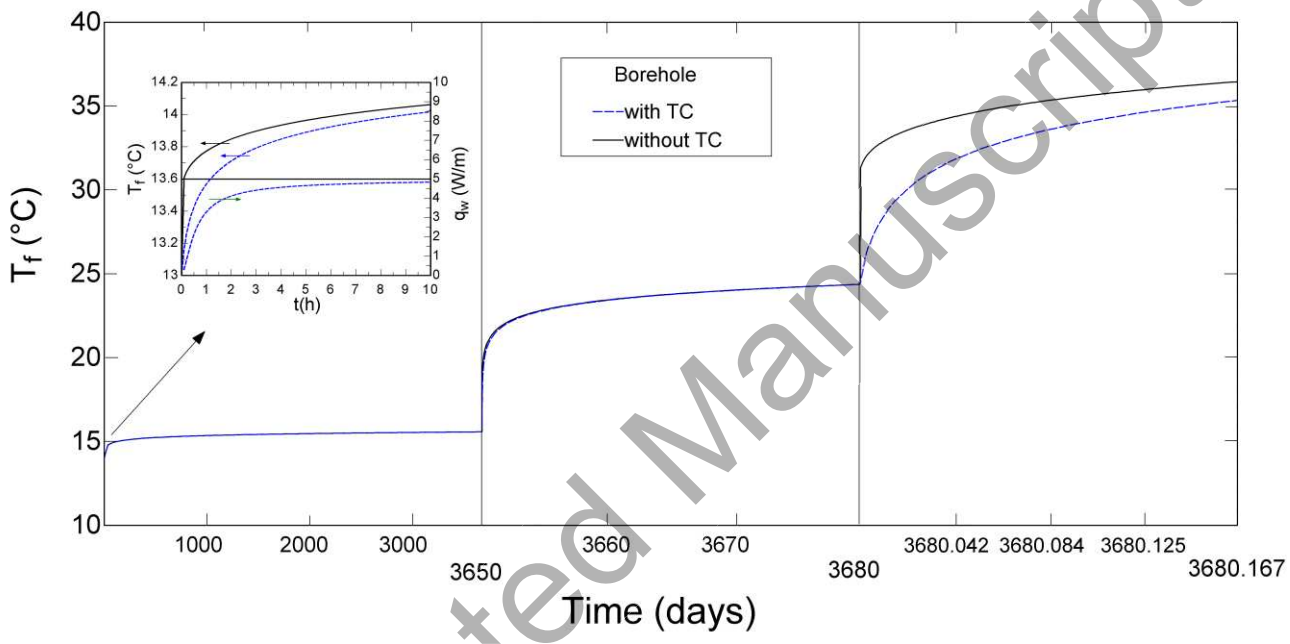


Figure 8 Evolution of the mean fluid temperature for cases with and without thermal capacity for three ground pulses applied over 10 years, 1 month and 4 hours.

Accepted Manuscript

CONCLUSION

A one-dimensional hybrid model is proposed to generate short-time g-functions for single U-tube boreholes. The two-pipe geometry is first converted into a single equivalent composite cylinder. This cylinder is discretized to numerically solve heat transfer in each layer while ground heat transfer is determined using the infinite cylindrical heat source solution. Both models are solved simultaneously at each time step. The proposed model is successfully validated against the experimental data of Beier et al. (2011).

When used to predict the outlet fluid temperature, the proposed 1D model compares favorably well with a more advanced 2D thermal-resistance-capacitance (TRCM) model if the fluid replacement rate is above one, i.e. for relatively high flow rates and/or short boreholes. Results for small replacement rates can be improved if the borehole thermal resistance is based on 4 , which accounts for the thermal short-circuit occurring between pipes. Nonetheless, these limits on the proposed model do not affect the mean fluid temperature, which is the basis for the generation of short time C- functions.

C-Functions are based on the fluid temperature instead of the wall temperature for traditional g-functions. In the short time domain, C-functions depend on four non-dimensional numbers: t Ł G4 , 0 , 0 , and [illegible]. For long times, borehole heat transfer is in steady-state and C-functions are equal to traditional g-functions. The proposed model is used to generate universal short-time C-functions curves (Figure 7) which can be used without the need to solve the proposed model.

In the application section of the paper, the ASHRAE sizing equation is modified to be based on C-functions. Then, the usefulness of the universal C-functions curves is illustrated in a typical borehole sizing problem. It is shown that the inclusion of borehole thermal capacity has a direct effect on the daily and monthly effective ground thermal resistances which reduces the required borehole length by a few percent.

ACKNOWLEDGMENTS

The financial support provided by the Natural Science and Engineering Research Council of Canada through a discovery grant and the Smart Net-Zero Energy Buildings Strategic Research Network is gratefully acknowledged.

NOMENCLATURE

a	=	discretization coefficient ($W.m^{-1}.K^{-1}$)	N	=	non-dimensional number
b	=	discretization coefficient	q	=	heat transfer rate per unit length (W/m)
B	=	borehole spacing (m)	Q	=	heat transfer rate (W)
C_p	=	specific heat capacity ($J.kg^{-1}.K^{-1}$)	r	=	radial distance from the borehole center (m)
D	=	buried depth of boreholes (m)	4	=	borehole thermal resistance ($m.K.W^{-1}$)
(	=	Fourier number	4	=	effective borehole thermal resistance

Accepted Manuscript

C = global g-function	(m.K.W^{-1})
h = film coefficient (W.m^{-2}.K^{-1})	t = time (h or s)
H = borehole length (m)	t_s = time scale (day)
k = thermal conductivity (W.m^{-1}.K^{-1})	t_c = time scale (h)
	T = temperature (°C)
	6 = mean fluid temperature (°C)
α = thermal diffusivity (m^2/s)	Δ = pipe thickness (m)
` = Response factor	ρ = density (kg.m^{-3})
δr = node spacing (m)	

SUBSCRIPTS

a = year	gt = grout	out = outside
b = borehole	C = based on g-function	p = pipe
c = convection	h = hour	P = node
eq = equivalent	in = inside	s = southern neighbor
f = fluid	m = month	w = wall
g = ground	n = northern neighbor	

SUPERSCRIPTS

0 =	based on previous timestep
* =	valid for short and long time

Accepted Manuscript

REFERENCES

ASHRAE. 2015. Chapter 34 – Geothermal Energy, ASHRAE Handbook - Applications, Atlanta, GA: ASHRAE.

Beier, R., M.D. Smith and J.D. Spitler. 2011. Reference data sets for vertical borehole ground heat exchanger models and thermal response test analysis. Geothermics 40: 79-85.

Beier. R.A. 2014. Transient heat transfer in a U-tube borehole heat exchanger. Applied Thermal Engineering 62: 256-266.

Bernier, M. 2014. Sizing and simulating bore fields using thermal response factors. Proceedings of the 11th IEA Heat Pump conference, Montreal (Quebec), Canada, May 2014. Paper KN.3.1.1.

Biglarian, H., M. Abbaspour and M. Hassan Saidi. 2017. A numerical model for transient simulation of borehole heat exchangers. Renewable Energy 104: 224-237.

Brussieux, Y. and M. Bernier. 2018. A hybrid model for generating short-time g-functions. Proceedings of the IGSHPA Research Conference, Stockholm, Sweden, September 2018, pp. 48-56.

Cimmino, M. and M. Bernier. 2013. Preprocessor for the generation of g-functions used in the simulation of geothermal systems, Proceedings of the 13th International IBPSA conference, 25-28 August, Chambery, France, pp.2675-2682.

Claesson, J. and S. Javed. 2011. An analytical method to calculate borehole fluid temperatures for time-scales from minutes to decades. ASHRAE annual conference, paper ML-11-C034.

Cooper, L.Y. 1976. Heating of a Cylindrical Cavity. International Journal of Heat and Mass Transfer 19: 575-577.

Cullin, J.R., J.D. Spitler, C. Montagud, F. Ruiz-Calvo, S.J. Rees, S.S. Naicker, P. Konečný, and L.E. Southard. 2015. Validation of vertical ground heat exchanger design methodologies. Science and Technology for the Built Environment 21(2):137–49.

De Rosa, M., F. Ruiz-Calvo, J.M. Corberan, C. Montagud and L. A. Tagliaco. 2014. Borehole modelling: a comparison between a steady-state model and a novel dynamic model in a real ON / OFF GSHP operation. 32nd UIT (Italian Union of Thermo-fluid-dynamics) Heat Transfer Conference/ Journal of Physics: Conference Series 547.

Eskilson, P. 1987. Thermal analysis of heat extraction boreholes. University of Lund, Sweden: Doctoral Thesis.

Godefroy, V and M. Bernier. 2014. A simple model to account for thermal capacity in boreholes. 11th IEA Heat Pump Conference, 12-16 May 2014, Montréal, Canada.

Gu, Y. and D. O'Neal. 1998. Development of an equivalent diameter expression for vertical U-Tubes used in ground-coupled heat pumps. ASHRAE Transactions, 104, 8.

He, M., S.J. Rees and L. Shao. 2010. Improvement of a Two-Dimensional Borehole Heat Exchanger Model. Proceedings of Conference: IESD PhD Conference: Energy and Sustainable Development. Leicester, UK, 21st May 2010.

Hellström, G. 1989. Duct Ground Heat Storage. Manual for Computer Code. Department of Mathematical Physics, University of Lund

Hellström, G. 1991. Ground Heat Storage, Thermal Analyses of Duct Storage Systems, Part I: Theory (thesis). Mathematical Physics, Lund.

Javed, S., J. Claesson and P. Fahlén. 2010. Analytical Modelling of Short-term Response of Ground Heat Exchangers in Ground Source Heat Pump Systems. 10th REHVA World Congress, Clima 2010, Antalya, Turkey, May 9-12.

Javed, S. and J. Claesson. 2011. New analytical and numerical solutions for the short-term analysis of vertical ground heat exchangers. ASHRAE Transaction 117(1): 3-12.

Javed, S. and J. Spitler. 2017. Accuracy of borehole thermal resistance calculation methods for grouted single U-tube ground heat exchangers. Applied Energy 187:790-806.

Kim, E.-J., M. Bernier, O. Cauret and J.-J. Roux. 2014. A hybrid reduced model for borehole heat exchangers over different time-scales and regions. Energy 77: 318-326.

Accepted Manuscript

Lamarche, L. 2015. Short-time analysis of vertical boreholes, new analytic solutions and choice of equivalent radius. International Journal of Heat and Mass Transfer 91: 800-807.

Lamarche, L. 2016. Short-time modelling of geothermal systems. 29th international conference on efficiency, cost, optimization, simulation and environmental impact of energy systems, Portoroz, Slovenia, June 19-23, Proceedings.

Lee, C.K. and H.N. Lam. 2008. Computer simulation of borehole ground heat exchangers for geothermal heat pump systems. Renewable Energy 33 (6) : 1286-1296.

Li, M. and A. C. Lai. 2013. Analytical model for short-time responses of ground heat exchangers with U-shaped tubes: Model development and validation. Applied Energy 104: 510-516.

Li, M. and A.C.K. Lai. 2015. Review of analytical models for heat transfer by vertical ground heat exchangers (GHEs): A perspective of time and space scales. Applied Energy 15: 178–191.

Li, M., P. Li, V. Chan and A. C. Lai. 2014. Full-scale temperature response function (G-function) for heat transfer by borehole ground heat exchangers (GHEs) from sub-hour to decades. Applied Energy 136: 197-205.

Li, M., X. Zhuo and G. Huang. 2017. Improvements on the American Society of Heating, Refrigeration, and Air-Conditioning Engineers Handbook equations for sizing borehole ground heat exchangers. Science and Technology for the Built Environment 23: 1267–1281.

Ma, W., M. Li, P. Li and A. C. Lai. 2015. New quasi-3D model for heat transfer in U-shaped GHEs (ground heat exchangers): Effective overall thermal resistance Energy 90: 578-587.

Minaei, A. and M. Maerefat. 2017. A new analytical model for short-term borehole heat exchanger based on thermal resistance capacity model. Energy and Buildings 146: 233–242.

Minaei, A. and M. Maerefat. 2017. Thermal resistance capacity model for short-term borehole heat exchanger simulation with non-stiff ordinary differential equations. Geothermics 70: 260–270.

Nian, Y-L. and W-L. Cheng. 2018. Analytical g-function for vertical geothermal boreholes with effect of borehole heat capacity. Applied Thermal Engineering 140: 733–744.

Pärisch, P., O. Mercker, P. Oberdorfer, E. Bertram, R. Tepe. and G. Rockendorf. 2015. Short-term experiments with borehole heat exchangers and model validation in TRNSYS. Renewable Energy 74: 471-477.

Patankar, S. V. 1980. Numerical heat transfer and fluid flow (2nd ed.). New York: McGraw-Hill.

Philippe, M., M. Bernier and D. Marchio. 2009. Validity ranges of three analytical solutions to heat transfer in the vicinity of single boreholes. Geothermics 38: 407-413

Rees, S.J. and M. He. 2013. A three-dimensional numerical model of borehole heat exchanger heat transfer and fluid flow. Geothermics 46: 1-13.

Rees, S. J. 2015. An extended two-dimensional borehole heat exchanger model for simulation of short and medium timescale thermal response. Renewable Energy 83: 518-526.

Accepted Manuscript

Ruiz-Calvo, F., M. De Rosa, P. Monzo, C. Montagud and J. Corberan. 2016. Coupling short-term (B2G model) and long-term (g-function) models for ground heat exchanger simulation in TRNSYS. Application in a real installation. App.Thermal Eng102: 720-732.

Ruiz-Calvo, F., De Rosa, M., Acuña, J., Corberán, J. and C. Montagud. 2015. Experimental validation of a short-term Borehole-to-Ground (B2G) dynamic model. Applied Energy 140: 210-223.

Shirazi, A. S. and M. Bernier. 2013. Thermal capacity effects in borehole ground heat exchangers. Energy and Buildings 67: 352-364.

Wetter, M. and A. Huber. 1997. TRNSYS Type 451 – Vertical Borehole Heat Exchanger – EWS model, https://trnsys.de/download/en/ts_type_451_en.pdf.

Xu, X. and J.D. Spitler. 2006. Modeling of Vertical Ground Loop Heat Exchangers with Variable Convective Resistance and Thermal Mass of the Fluid. Proceedings of the 10th Int. Conference on Thermal Energy Storage-Ecostock 2006, Pomona, NJ.

Yang, Y. and M. Li. 2014. Short-time performance of composite-medium line-source model for predicting responses of ground heat exchangers with single U-shaped tube. International Journal of Thermal Sciences 82: 130-137.

Yavuzturk, C. and J.D. Spitler. 1999. A short time step response factor model for vertical ground loop heat exchangers. ASHRAE Transactions. 105(2): 475-485.

Yavuzturk, C, A.D. Chiasson and J.E. Nydahl. 2009. Simulation model for ground loop heat exchangers. ASHRAE Transactions 115(2):45-59.

Accepted Manuscript